

# The $\beta^+$ -electron capture decay of $^{73}\text{Kr}$

Ch. Miehé<sup>1</sup>, Ph. Dessagne<sup>1</sup>, Ch. Pujol<sup>1</sup>, G. Walter<sup>1</sup>, B. Jonson<sup>2</sup>, M. Lindroos<sup>3</sup>, and The ISOLDE Collaboration<sup>3</sup>

<sup>1</sup> Institut de Recherches Subatomiques, UMR7500, CNRS-IN2P3 et Université Louis Pasteur, BP28, F-67037 Strasbourg Cedex 2, France

<sup>2</sup> Chalmers University of Technology, Göteborg, Sweden

<sup>3</sup> CERN, CH-1211 Geneva, Switzerland

Received: 17 September 1998 / Revised version: 25 January 1999

Communicated by J. Äystö

**Abstract.** The  $\beta^+$  – electron capture decay of  $^{73}\text{Kr}$ , produced at the ISOLDE CERN facility, has been studied by  $\beta$ -delayed proton and gamma emission. The established decay scheme involves 15 up to now unreported gamma emitting levels in  $^{73}\text{Br}$ . The total proton branching ratio has been measured to be  $0.0025 \pm 0.0003$ . From this work, a spin and parity  $3/2^-$  is assigned to the  $^{73}\text{Kr}$  ground state, on the basis of the allowed  $\beta$  branch to the  $^{73}\text{Br}$   $J^\pi = 1/2^-$  ground state and the feeding of the  $5/2^+$  level located at 286 keV in  $^{73}\text{Br}$ .

**PACS.** 21.10.Hw Spin, parity, and isobaric spin – 23.20.Lv Gamma transitions and level energies – 23.40.Hc Relation with nuclear matrix elements and nuclear structure – 27.50.+e  $59 \leq A \leq 89$

## 1 Introduction

The proton rich nuclei in the  $A=70$  mass region are located close to the  $N=Z$  line, in an area where large quadrupole deformations, triaxiality, shape coexistences and shape transitions have been predicted and in many cases observed. In mass 73, a decisive contribution to the characterization of the  $^{73}\text{Br}$  excited levels has been brought in by the elaborate in beam work of J. Heese et al. [1, 2]. From their  $\gamma$ -ray measurements, evidence for two rotational bands of negative parity, and for one of positive parity has been found. The authors also established the existence of a low lying level at 27 keV, from conversion electron measurements, and determined the multipolarity of several transitions in the band head region. The spin and parity pattern of most of the low lying levels in  $^{73}\text{Br}$  could so be inferred from the previously known  $J^\pi = 1/2^-$  value of the  $^{73}\text{Br}$  ground state [3].

The  $\beta^+$  – EC decay mode, with the attached spin and parity selectivity, yields an experimental access to low spin states that cannot be reached via fusion evaporation reactions. Its study is therefore essential for a comprehensive insight into nuclear structure. Only partial information was obtained from earlier work on the radioactive decay of the  $^{73}\text{Kr}$  isotope [4–7], and investigation under better experimental conditions became of interest with respect to several points. Among these, the determination of the spin and parity of the  $^{73}\text{Kr}$  ground state and the location of unreported low spin levels in  $^{73}\text{Br}$  up to the proton separation energy. In addition, improvement in the detec-

tion of the delayed proton emission was expected to offer more precise insight than previously obtained [6, 7] into the population of unbound states of the emitter.

## 2 Experimental procedure

The  $^{73}\text{Kr}$  isotope was produced at the ISOLDE II facility, by bombarding a niobium target with the  $2\mu\text{A}$  600 MeV proton beam of the CERN synchrocyclotron. A typical yield was  $3.10^5$  atoms per second.

The mass separated ion beam was steered to a tape transport system serving two independent counting stations operated simultaneously. The first one, located at the collection point, was devoted to  $\gamma$  ray measurements, and equipped with a  $4\pi$   $\beta$  detector and two germanium counters of 33% and 80% efficiency, covering 0.1–2.2 and 0.1–5.1 MeV energy ranges respectively.  $\beta$ - $\gamma$  and  $\gamma$ - $\gamma$  coincidence measurements have been performed and multi-spectra have been registered in 14 s, 30 s and in 120 s time bins. The second station was dedicated to direct proton, proton-X and proton- $\gamma$  coincidence measurements. The delayed protons were detected by a water cooled silicon counter (280 mm<sup>2</sup> sensitive area, 100  $\mu\text{m}$  thickness) subtending a solid angle of 19% of  $4\pi$  sr. A 17 keV FWHM was obtained on line. In order to establish the proton decay to excited levels in the daughter nucleus, proton- $\gamma$  coincidence measurements were carried out with a Ge detector of 80% efficiency. A 300 mm<sup>2</sup> Si(Li) counter faced the proton detector in a close geometry, allowing efficient

proton – X-rays coincidence and low energy gamma ray measurements. It covered a solid angle of 1.6% of  $4\pi$  sr and its energy resolution was 270 eV at 6 keV.

Calibration of the particle spectra was achieved with the alpha emitters  $^{239}\text{Pu}$ ,  $^{241}\text{Am}$  and  $^{244}\text{Cm}$ . The thickness of the entrance window of the detector and the relatively lower ionization power of the protons with regard to alpha particles [8] were taken into account. Efficiencies of the gamma and X-ray detectors were determined with  $^{56}\text{Co}$ ,  $^{152}\text{Eu}$  and  $^{133}\text{Ba}$  standard sources, the last one being used for the absolute intensity calibration.

### 3 Results

A new estimate of the  $^{73}\text{Kr}$  half-life is inferred from the multispectra registered in different time bins of the  $\text{K}_\alpha$  X-ray of  $^{73}\text{Br}$  and the delayed proton distributions – after subtraction of the exponentially shaped beta background. The weighted average of these measurements yields a value of  $29.0 \pm 1.0$  s which is in agreement with two of the previously reported determinations [5, 7].

#### 3.1 $\beta$ decay to ground and $\gamma$ deexciting states in $^{73}\text{Br}$

In the earlier works on the  $^{73}\text{Kr}$   $\beta$ - $\gamma$  decay [4, 5], due to low production yields, only the most prominent gamma rays could be observed and no coincidence measurements could be performed. The high production rate achieved at ISOLDE, together with an efficient gamma detection, provided access to more comprehensive information on gamma emitting levels in  $^{73}\text{Br}$ .

We have included in Table 1 all the  $\gamma$ -rays assigned to the decay of  $^{73}\text{Kr}$  on the basis of the multispectra ratios and the coincidence measurements. The gamma line at 26.9 keV, expected from the work of J. Heese et al. [2], is observed for the first time. The proposed decay scheme extends up to 3469 keV of excitation energy, with five levels located above the proton separation energy (Fig. 1). Each level – one excepted – relies on at least two deexciting transitions or an established cascade. The gamma-ray spectra registered in coincidence with the 178 keV line are shown in Fig. 2. From the observed radiative emission, the existence of 15 up to now unreported states is deduced. Gamma branchings established for the  $^{73}\text{Br}$  states populated in the beta decay are quoted in Table 2.

The existence of excited levels at 303, 329 and 391 keV previously proposed [4] is no longer supported. Indeed, the 303 keV gamma line is seen in coincidence with the lines originating from the 178 keV state, and is therefore attributed to the deexcitation of the 481 keV state, in agreement with the work of J. Heese et al. [1]. The line at 329 keV, interpreted as a ground state transition from a level of the same energy is not present in our spectra. Our results confirm the attribution of the 213 keV line to the  $240 \rightarrow 27$  keV transition [1, 2]. Indeed, from its intensity in the direct spectrum, one would expect  $\gamma - \gamma$  coincidences

if the 213 keV line would deexcite the 391 keV state as it has been suggested [4]. In addition we observe this line in coincidence with the 183 keV line feeding the 240 keV level. For the radiative decay of the state at 681 keV, established by J. Heese et al. [2] to have spin and parity  $7/2^-$ , only the 503 and 654 keV lines are present in our spectra and the 207 keV transition reported by these authors is missing.

A reliable estimate of the  $\beta$  transition to the  $^{73}\text{Br}$  ground state is obtained from a comparison of the parent and the daughter activities at the upper counting station, towards which the collected sources are moved each 30 s and where no accidental buildup of  $^{73}\text{Br}$  activity on a collimator can occur. One has to mention that no bromine is present in the chemically pure beam. The measurement is based on a quantitative comparison of the intensities of the 65 keV transition in  $^{73}\text{Se}$  and the 62 keV transition in  $^{73}\text{Br}$ . Their relative intensity depends on the radioactive filiation law, on the time conditions governing the measurement and their weight in the relevant beta decay schemes. The intensity of the 65 keV transition in  $^{73}\text{Se}$  from the  $^{73}\text{Br}$  beta decay is 50 per 100 decays, according to reference [9]. The 62 and 65 keV lines are registered with the high efficiency X-ray detector (Fig. 3) and are both of magnetic dipole type [9]. To account for the intensity of the 65 keV line, the intensity of the 62 keV has to be 4.6% of the  $^{73}\text{Kr}$  decay. According to the decay scheme we have established, a beta feeding of the ground and first excited states summing up to  $40 \pm 12\%$  is inferred. This value is confirmed by the relative intensity of the main gamma lines in  $^{73}\text{Br}$  and  $^{73}\text{Se}$  ranging from 27 to 1976 keV. The 27 keV line has been established to be of E2 character [2] and is therefore strongly converted. The conversion coefficient has been calculated with the F. Rösler and coworkers [10] formula from which a value of 103.6 has been obtained. Taking into account the error bars on the involved quantities, an upper limit of 8.6% is found for the feeding of the 27 keV level from the  $\gamma$ -in  $\gamma$ -out imbalance. The different beta branching ratios being summed up to 100%, the ground state feeding finally restricts to  $27 < x < 45\%$ . In the earlier estimate by C. Davis et al. [4], only about 50% of the beta decay intensity we observed has been seen and a 0% of the beta ground state feeding is suggested. This discrepancy can be related to the evaluation of the intensity of the 65 keV transition.

The beta branchings,  $\log ft$  values and the corresponding reduced transition probabilities  $B(\text{GT})$  to the gamma emitting levels are quoted in Table 3. The  $ft$  values are calculated with  $T_{1/2} = 29 \pm 1$  s and using the mass values of G. Audi and A. H. Wapstra [11]. The  $\log ft$  values are uniformly distributed in the band head region and no noticeable difference is observed between the beta feeding of the 286( $5/2^+$ ) and 481( $5/2^-$ ) keV levels which are members of positive and negative parity bands with a large prolate deformation ( $\beta_2 \sim 0.37$ ) [1]. At high excitation energy, two transitions of allowed character take place to the 3017 keV and 3462 keV levels. The  $B(\text{GT})$  values are defined as  $3880/ft$ .

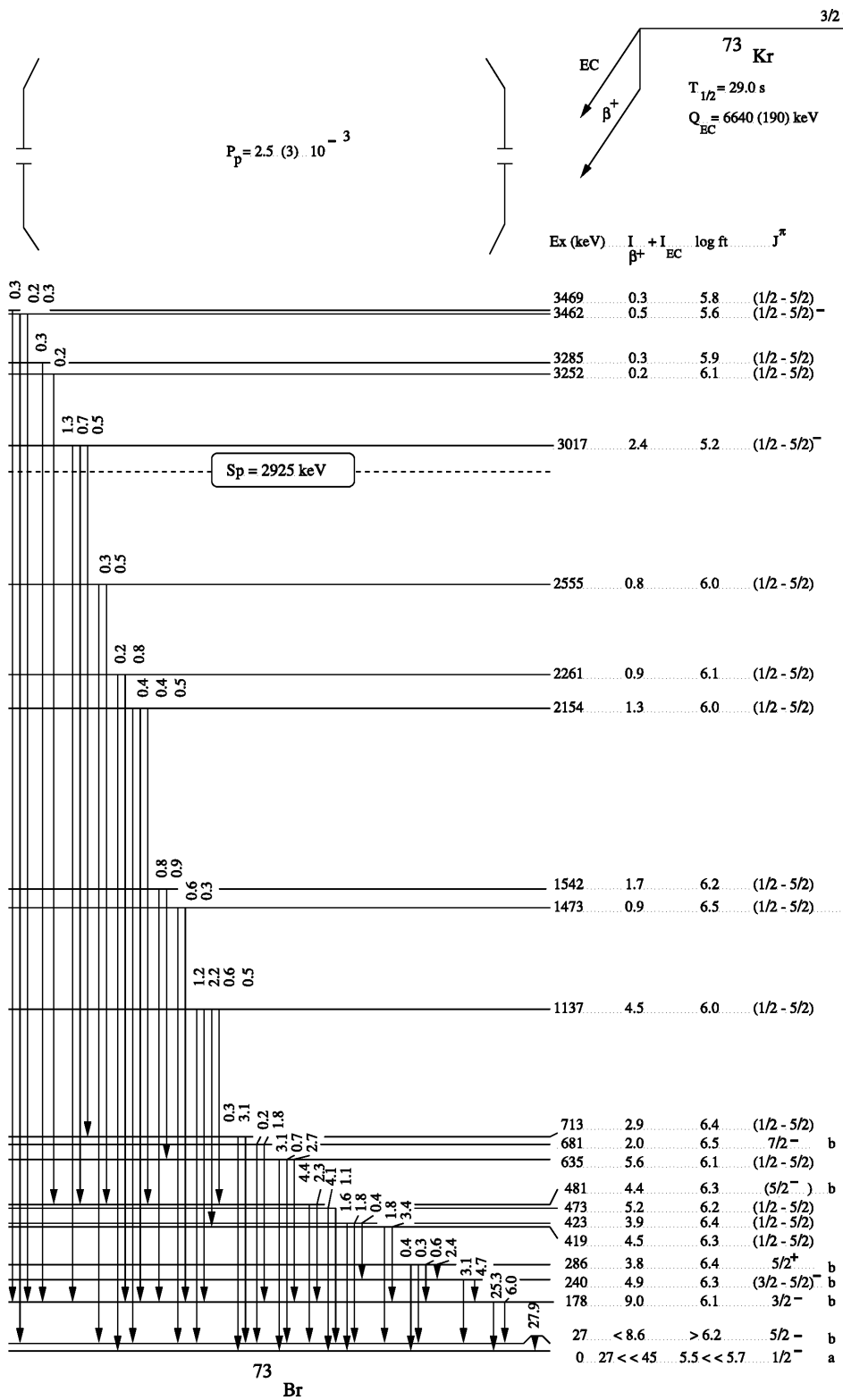


Fig. 1. Proposed decay scheme for  $^{73}\text{Kr}$ . Spin and parity assignments labelled by a and b are from references 3 and 2 respectively

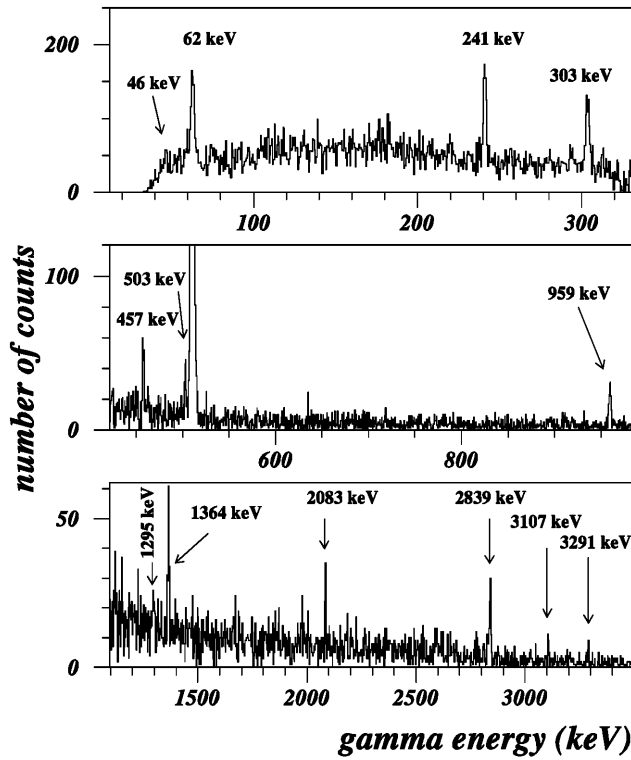


Fig. 2. Gamma ray spectra registered in coincidence with the 178 keV gamma line. The two upper spectra are obtained with the 33% efficiency germanium detector, the lower one with the 80% efficiency germanium counter

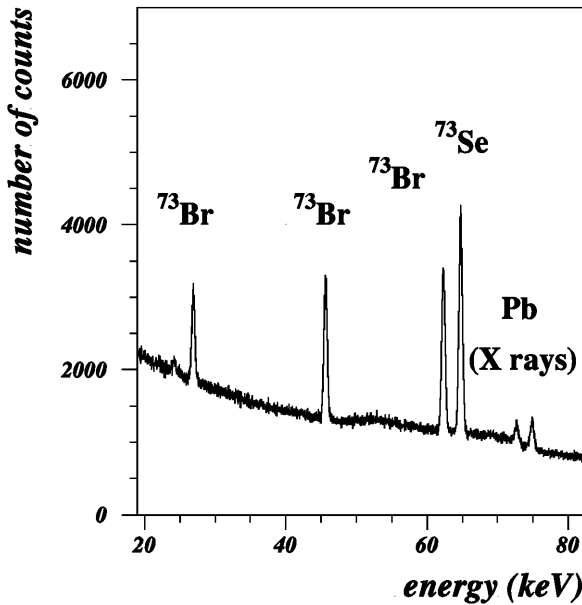


Fig. 3. Low energy  $\gamma$  ray spectrum registered with the high resolution X-ray counter

Table 1. Energies, relative intensities and coincident  $\gamma$ -rays of the transitions in  $^{73}\text{Br}$  following the  $\beta^+$  – EC decay of  $^{73}\text{Kr}$

$E_\gamma$ (keV)	$I_{\gamma+\text{IC}}$	Coincident transitions	$E_i$ (keV)	$E_f$ (keV)
$26.9 \pm 0.1$	$110.5 \pm 24.0$		27	0
$45.6 \pm 0.1$	$9.5 \pm 2.1$	62, 178	286	240
$62.4 \pm 0.1$	$18.6 \pm 4.1$	46, 151, 178, 183	240	178
$108.0 \pm 0.6$	$2.6 \pm 1.3$		286	178
$151.2 \pm 0.3$	$23.9 \pm 2.7$	62,241,303,457, 718,959,1364, 2839	178	27
$178.0 \pm 0.3$	100	46,62,241,303, 457,503,959, 1295,1364,2083, 2839,3107,3291	178	0
$183.1 \pm 0.6$	$1.8 \pm 1.1$	62, 213	423	240
$213.3 \pm 0.4$	$12.1 \pm 1.4$	183	240	27
$241.0 \pm 0.3$	$13.4 \pm 1.5$	151, 178, 718	419	178
$259.0 \pm 0.4$	$1.1 \pm 0.1$		286	27
$286.8 \pm 0.4$	$1.8 \pm 0.2$		286	0
$303.4 \pm 0.3$	$9.3 \pm 1.1$	151, 178	481	178
$391.9 \pm 0.4$	$7.0 \pm 0.8$	(718)	419	27
$396.4 \pm 0.4$	$7.2 \pm 0.8$		423	27
$423.4 \pm 0.3$	$6.4 \pm 0.7$		423	0
$446.4 \pm 0.7$	$4.3 \pm 0.5$		473	27
$454.3 \pm 0.5$	$17.4 \pm 3.2$	656, 1673	481	27
$457.2 \pm 0.5$	$10.8 \pm 2.4$	151, 178	635	178
$473.4 \pm 0.3$	$16.2 \pm 1.9$		473	0
$503.0 \pm 0.4$	$7.1 \pm 3.6$	178	681	178
$608.5 \pm 0.4$	$2.7 \pm 0.3$		635	27
$635.1 \pm 0.3$	$12.1 \pm 1.4$		635	0
$654.2 \pm 0.5$	$0.9 \pm 0.2$		681	27
$656.2 \pm 0.5$	$1.9 \pm 0.4$	454	1137	481
$686.1 \pm 0.4$	$12.2 \pm 1.4$	2304	713	27
$713.4 \pm 0.4$	$1.2 \pm 0.2$		713	0
$718.3 \pm 0.4$	$2.5 \pm 0.3$	178, 241, 392	1137	419
$907.0 \pm 0.4$	$3.4 \pm 0.4$	608, 635	1542	635
$959.6 \pm 0.3$	$8.8 \pm 1.0$	151,178	1137	178
$1110.6 \pm 0.3$	$4.7 \pm 0.5$		1137	27
$1295.2 \pm 0.5$	$1.3 \pm 0.2$	178	1473	178
$1364.4 \pm 0.4$	$3.2 \pm 0.4$	151,178	1542	178
$1445.7 \pm 0.6$	$2.2 \pm 0.3$		1473	27
$1672.9 \pm 0.7$	$1.8 \pm 0.2$	303, 454	2154	481
$1975.7 \pm 0.6$	$1.7 \pm 0.2$	178	2154	178
$2073.8 \pm 0.6$	$2.1 \pm 0.2$	454	2555	481
$2083.1 \pm 0.6$	$3.0 \pm 0.3$	178	2261	178
$2126.9 \pm 0.6$	$1.6 \pm 0.2$		2154	27
$2262.0 \pm 0.7$	$0.6 \pm 0.1$		2261	0
$2303.7 \pm 0.6$	$2.0 \pm 0.2$	686	3017	713
$2527.9 \pm 0.6$	$1.0 \pm 0.1$		2555	27
$2537.0 \pm 0.6$	$2.6 \pm 0.3$	454	3017	481
$2770.8 \pm 0.7$	$0.9 \pm 0.1$	454	3252	481
$2838.6 \pm 0.6$	$5.0 \pm 0.6$	178	3017	178
$3107.0 \pm 0.7$	$1.4 \pm 0.2$	178	3285	178
$3284.4 \pm 0.7$	$1.3 \pm 0.2$	(151), 178	3462	178
$3291.0 \pm 0.7$	$1.0 \pm 0.1$	178	3469	178
$3434.9 \pm 0.8$	$0.7 \pm 0.1$		3462	27

**Table 2.** Transition branching ratios in  $^{73}\text{Br}$ 

$E_x(\text{keV})$	$E_\gamma(\text{keV})$	$I_{\gamma+IC}(\%)$
$26.9 \pm 0.1$	27	100
$178.0 \pm 0.2$	151	$19 \pm 2$
	178	$81 \pm 2$
$240.4 \pm 0.2$	62	$60 \pm 5$
	213	$40 \pm 5$
$286.1 \pm 0.2$	46	$64 \pm 7$
	108	$17 \pm 8$
	259	$7 \pm 2$
	287	$12 \pm 2$
$419.0 \pm 0.2$	241	$66 \pm 3$
	392	$34 \pm 3$
$423.4 \pm 0.2$	183	$12 \pm 6$
	396	$46 \pm 4$
	423	$42 \pm 4$
$473.4 \pm 0.3$	446	$21 \pm 2$
	473	$79 \pm 2$
$481.4 \pm 0.3$	303	$35 \pm 4$
	454	$65 \pm 4$
$635.2 \pm 0.2$	457	$42 \pm 5$
	608	$11 \pm 1$
	635	$47 \pm 4$
$681.1 \pm 0.3$	503	$89 \pm 6$
	654	$11 \pm 6$
$713.2 \pm 0.3$	686	$91 \pm 1$
	713	$9 \pm 1$
$1137.5 \pm 0.2$	656	$11 \pm 2$
	718	$14 \pm 1$
	960	$49 \pm 2$
	1111	$26 \pm 2$
$1473.1 \pm 0.3$	1295	$36 \pm 3$
	1446	$64 \pm 3$
$1542.3 \pm 0.2$	907	$52 \pm 3$
	1364	$48 \pm 3$
$2154.0 \pm 0.3$	1673	$36 \pm 3$
	1976	$34 \pm 3$
	2127	$30 \pm 2$
$2261.5 \pm 0.4$	2083	$82 \pm 2$
	2262	$18 \pm 2$
$2555.1 \pm 0.4$	2074	$67 \pm 3$
	2528	$33 \pm 3$
$3017.4 \pm 0.4$	2304	$20 \pm 2$
	2537	$28 \pm 2$
	2839	$52 \pm 3$
$3252.2 \pm 0.5$	2771	100
$3285.1 \pm 0.5$	3107	100
$3462.3 \pm 0.4$	3284	$66 \pm 3$
	3435	$34 \pm 3$
$3469.1 \pm 0.5$	3291	100

### 3.1.1 Spin and parity of the $^{73}\text{Kr}$ ground state

For the decay to the  $^{73}\text{Br}$  ground state, the  $\log ft$  value inferred from our measurements lies in between 5.5 and 5.7, corresponding to an allowed transition, with  $\Delta J = 0, 1$  and no parity change. According to the established  $J^\pi = 1/2^-$  value of  $^{73}\text{Br}$  [3], this implies a spin and parity  $1/2^-$  or  $3/2^-$  for the  $^{73}\text{Kr}$  ground state. The beta decay to the  $5/2^+$  level at 286 keV with  $\log ft=6.4$  restricts to  $3/2^-$  the

angular momentum of  $^{73}\text{Kr}$  g.s. as this value rules out the occurrence of a  $\Delta J = 2$  transition with a parity change, and thus also a value  $1/2$  for the ground state angular momentum. From our decay scheme the beta feeding of the 681 keV ( $J^\pi = 7/2^-$ ) level is weak with a large gamma imbalance error bar ( $2.0 \pm 0.9\%$ ). For a  $3/2^- \rightarrow 7/2^-$  transition, of second forbidden non unique character ( $\Delta J = 2$ , no parity change), an upper limit of the transition intensity is expected to be  $2 \cdot 10^{-4}$  [12]. No gamma feeding of the 681 keV level is seen from our  $\gamma$ - $\gamma$  coincidence data down to the 0.3% intensity. The  $\gamma$  feeding of this level from the upper states by several transitions all of them weaker than 0.3% cannot be excluded. Indeed, in the beta decay, gamma rays are emitted that are under the threshold of experimental sensitivity due to their intensity and the detection efficiency. This fact leads to an overestimate of the beta feedings of the low lying levels and an underestimate for the upper levels. This experimental bias can be evaluated by simulating the  $\gamma$  spectrum resulting from the statistical beta decay with an appropriate threshold for the gamma detection. An enhancement of the order of one percent is obtained for levels located below 1 MeV excitation energy in the daughter nucleus. Therefore the  $\beta$  feeding of the 681 keV level can be considered compatible with zero.

No direct spin and parity determination has up to now been performed for the ground state of  $^{73}\text{Kr}$ . From an analysis of previous beta decay data, J. Heese et al. [2], proposed a spin and parity  $5/2^-$  for the  $^{73}\text{Kr}$  ground state. In this investigation the feeding of the 27 keV level - unobserved in the decay - and the ground state feeding had to be treated together. From our measurements, the beta branchings to these two states could be evaluated separately. The resulting intensity of the ground state branch excludes the suggested  $5/2^-$  value. Our  $J^\pi=3/2^-$  assignment supports the conclusions of the in beam work of M. Satteson et al. [13] and D.M. Moltz et al. [14] based on both the similarity of the  $^{75}\text{Kr}$  and  $^{73}\text{Kr}$  excited bands and on the theoretical expectations for a prolate deformation.

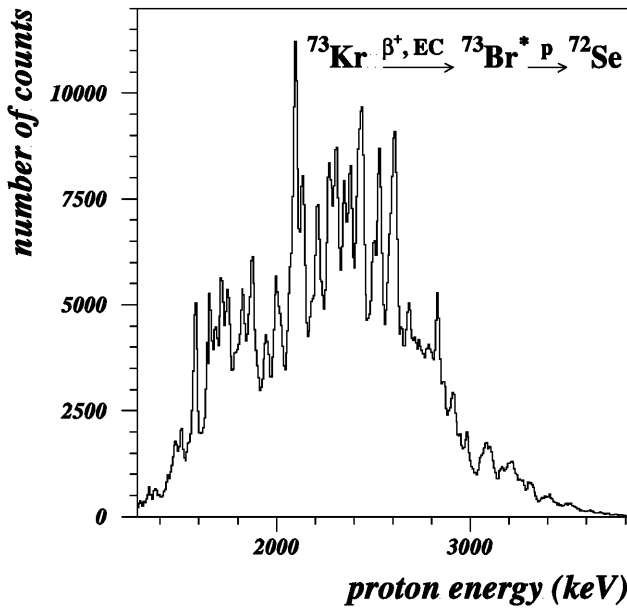
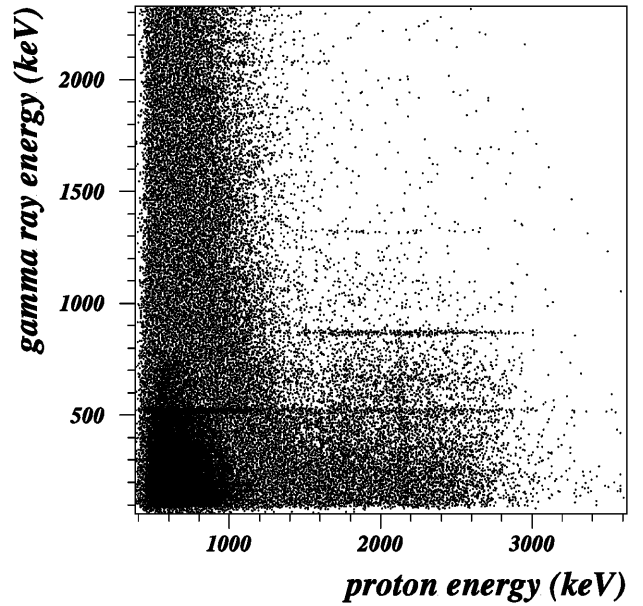
### 3.2 Delayed proton emission

The total proton branching ratio  $P_p$  has been determined by comparing, after suitable efficiency corrections, the number of protons detected - estimated after subtraction of the beta background in the particle spectrum - with the number of counts in the 959, 686, 635 keV lines observed with the Ge counter and the 46 and 63 keV lines seen by the X-ray detector. The weighted mean of the obtained  $P_p$  values is equal to  $0.0025 \pm 0.0003$ . This new value is of the same order of magnitude as the previously reported one [7] and remains noticeably higher than that expected from the calculations i.e.  $3.6 \cdot 10^{-4}$  [6].

The beta background subtracted proton energy spectrum presents well marked structures in the distribution that extends up to 3.8 MeV (Fig. 4). Two gamma lines are detected in coincidence with the delayed protons, as

**Table 3.**  $\beta$  branching,  $\log f_{0t}$  and B(GT) values in the decay of  $^{73}\text{Kr}$  to ground and  $\gamma$  emitting levels of  $^{73}\text{Br}$ 

$E_x(\text{keV})$	$I_\beta(\%)$	$\log f_{0t}$	$B(\text{GT}) \times 10^3$	$J^\pi$
0.0	$26.6 < x < 44.8$	$5.5 < x < 5.7$	$8.2 < x < 13.9$	$1/2^-$
26.9	$< 8.6$	$> 6.2$	$< 2.7$	$5/2^-$
178.0	$9.0 \pm 2.3$	$6.1 (-0.2 + 0.2)$	$3.2 \pm 1.2$	$3/2^-$
240.4	$4.9 \pm 1.1$	$6.3 (-0.2 + 0.2)$	$1.9 \pm .6$	$(3/2, 5/2)^-$
286.1	$3.8 \pm 0.6$	$6.4 (-0.2 + 0.1)$	$1.5 \pm .4$	$5/2^+$
419.0	$4.5 \pm 0.5$	$6.3 (-0.1 + 0.1)$	$2.0 \pm .5$	$(1/2, 3/2, 5/2)$
423.4	$3.9 \pm 0.5$	$6.4 (-0.1 + 0.1)$	$1.7 \pm .5$	$(1/2, 3/2, 5/2)$
473.4	$5.2 \pm 0.6$	$6.2 (-0.1 + 0.1)$	$2.4 \pm .6$	$(1/2, 3/2, 5/2)$
481.4	$4.4 \pm 0.8$	$6.3 (-0.2 + 0.1)$	$2.0 \pm .6$	$5/2^-$
635.2	$5.6 \pm 0.8$	$6.1 (-0.1 + 0.1)$	$3.0 \pm .8$	$(1/2, 3/2, 5/2)$
681.1	$2.0 \pm 0.9$	$6.5 (-0.3 + 0.2)$	$1.1 \pm .6$	$7/2^-$
713.2	$2.9 \pm 0.4$	$6.4 (-0.1 + 0.1)$	$1.7 \pm .5$	$(1/2, 3/2, 5/2)$
1137.5	$4.5 \pm 0.5$	$6.0 (-0.1 + 0.1)$	$4.0 \pm 1.1$	$(1/2, 3/2, 5/2)$
1473.1	$0.9 \pm 0.1$	$6.5 (-0.1 + 0.1)$	$1.1 \pm .3$	$(1/2, 3/2, 5/2)$
1542.3	$1.7 \pm 0.2$	$6.2 (-0.1 + 0.1)$	$2.2 \pm .6$	$(1/2, 3/2, 5/2)$
2154.0	$1.3 \pm 0.1$	$6.0 (-0.2 + 0.1)$	$3.6 \pm 1.1$	$(1/2, 3/2, 5/2)$
2261.5	$0.9 \pm 0.1$	$6.1 (-0.2 + 0.2)$	$2.9 \pm .9$	$(1/2, 3/2, 5/2)$
2555.1	$0.8 \pm 0.1$	$6.0 (-0.2 + 0.2)$	$3.8 \pm 1.3$	$(1/2, 3/2, 5/2)$
3017.4	$2.4 \pm 0.2$	$5.2 (-0.2 + 0.2)$	$24 \pm 8$	$(1/2, 3/2, 5/2)^-$
3252.2	$0.23 \pm 0.02$	$6.1 (-0.2 + 0.2)$	$3.3 \pm 1.2$	$(1/2, 3/2, 5/2)$
3285.1	$0.35 \pm 0.03$	$5.9 (-0.2 + 0.2)$	$5.4 \pm 2.0$	$(1/2, 3/2, 5/2)$
3462.3	$0.50 \pm 0.05$	$5.6 (-0.2 + 0.2)$	$11 \pm 4$	$(1/2, 3/2, 5/2)^-$
3469.1	$0.25 \pm 0.03$	$5.8 (-0.2 + 0.2)$	$5.5 \pm 2.2$	$(1/2, 3/2, 5/2)$

**Fig. 4.**  $\beta$  delayed proton spectrum of  $^{73}\text{Kr}$  resulting from 25 hours of accumulation. The exponential  $\beta$  background has been subtracted**Fig. 5.** Proton – gamma coincidence spectrum

shown in Fig. 5. They indicate that protons feed the levels located at  $0.86(2^+)$  and  $1.31(2^+)$  MeV in  $^{72}\text{Se}$ . The proton spectrum in coincidence with the 0.86 MeV  $\gamma$ -line is shown in Fig. 6. No proton decay is observed to the 0.94 MeV ( $0^+$ ) level which is most likely the experimental counterpart of the  $0_2^+$  triaxially deformed isomeric state predicted by M. Girod and coworkers in the HFB for-

malism [15]. Indeed, a significative population would be signed by the subsequent 73 keV  $\gamma$ -transition detected in the high efficiency X-ray counter. A quantitative analysis of our proton spectra indicates that delayed proton emission proceeds with an intensity of  $0.5 \pm 0.1\%$  of the total proton decay via the 1.31 MeV level. The feeding of the level at 0.86 MeV amounts to  $19.1 \pm 1.5\%$ . The ground

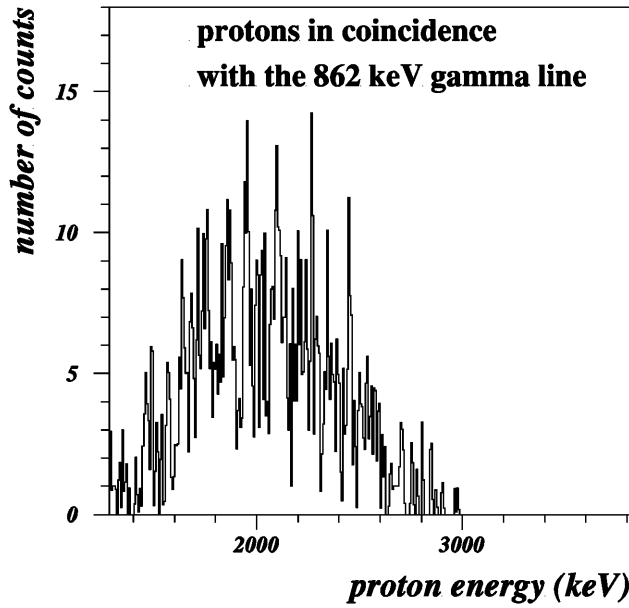


**Fig. 6.**  $\beta$  delayed proton spectrum registered in coincidence with the 862 keV transition in  $^{72}\text{Se}$  and with  $\beta$  background subtracted

state proton transitions amount to  $80.4 \pm 1.5\%$  and no population of the  $4^+$  state at 1.63 MeV is observed. On the basis of penetrability calculations, protons are expected to feed the ground and first excited state of  $^{72}\text{Se}$  in the ratio 0.8 to 0.2.

The quantitative analysis of the proton energy spectrum is performed in terms of the two main components to the ground and first excited state of  $^{72}\text{Se}$ . The distribution of the protons feeding the 0.86 MeV state in  $^{72}\text{Se}$  is obtained from the proton-gamma coincidence measurement after suitable correction for gamma efficiency. The proton energy distribution to the  $^{72}\text{Se}$  ground state, resulting from the direct spectrum after subtraction of the  $2^+$  component, is analysed in 42 proton groups according to the structure of the histogram. The corresponding excitation energies in  $^{73}\text{Br}$  are deduced from the emitted particle energy, the proton separation energy of  $2925 \pm 130$  keV [11] and by taking into account the recoil of the emitter. We have quoted in Table 4 the  $\beta^+$ -EC branching ratio,  $\log ft$  and B(GT) values for the so defined energy bins, summing up the two contributions to the ground and first excited states in  $^{72}\text{Se}$ . The reported values account only for the delayed proton channel, the competing gamma decay escaping our observation. Branching ratios and B(GT) values have therefore to be taken as lower limits, while the  $\log ft$  values should be taken as upper limits for the excitation energy domains.

In the mass region under study, the excitation energy range open to delayed proton emission is located in between the experimentally well resolved region and the continuum. A statistical analysis of the relevant data then allows a determination of the mean level spacing and of the partial decay widths on the proton rich side, far off stability. These aspects for  $^{73}\text{Br}$  will be discussed in a separate

**Table 4.** Excitation energy centroids,  $\beta$  branchings,  $\log f_0 t$  and B(GT) values for  $^{73}\text{Kr}$  delayed proton emission to  $^{72}\text{Se}$  g.s. and first excited state. The quantity  $r$  indicates the relative amount of proton decays to the ground state of  $^{72}\text{Se}$

$E_x(\text{MeV})$	$I_\beta(\%) \times 10^{+3}$	$r$	$\log f_0 t$	B(GT) $\times 10^3$
4.28	$0.3 \pm 0.2$	1.00	7.9 (-0.4 + 0.4)	$.04 \pm .03$
4.33	$0.6 \pm 0.1$	1.00	7.6 (-0.3 + 0.3)	$.09 \pm .04$
4.38	$0.7 \pm 0.2$	1.00	7.6 (-0.4 + 0.3)	$.11 \pm .06$
4.43	$0.7 \pm 0.3$	1.00	7.5 (-0.4 + 0.3)	$.12 \pm .07$
4.46	$1.6 \pm 0.2$	1.00	7.1 (-0.3 + 0.3)	$.31 \pm .14$
4.50	$1.1 \pm 0.2$	1.00	7.2 (-0.3 + 0.3)	$.23 \pm .11$
4.53	$4.3 \pm 0.6$	1.00	6.6 (-0.3 + 0.3)	$.96 \pm .43$
4.60	$4.2 \pm 0.6$	1.00	6.5 (-0.3 + 0.3)	$1.1 \pm .5$
4.64	$3.6 \pm 0.5$	1.00	6.6 (-0.3 + 0.3)	$1.1 \pm .5$
4.67	$3.5 \pm 0.5$	1.00	6.6 (-0.3 + 0.3)	$1.1 \pm .5$
4.71	$2.7 \pm 0.5$	1.00	6.6 (-0.3 + 0.3)	$.9 \pm .4$
4.74	$2.7 \pm 0.4$	1.00	6.6 (-0.3 + 0.3)	$1.0 \pm .4$
4.78	$4.1 \pm 0.6$	1.00	6.4 (-0.2 + 0.2)	$1.7 \pm .7$
4.83	$6.3 \pm 0.9$	1.00	6.1 (-0.2 + 0.2)	$2.9 \pm 1.2$
4.89	$3.4 \pm 0.6$	1.00	6.3 (-0.2 + 0.3)	$1.8 \pm .8$
4.96	$7.7 \pm 1.1$	1.00	5.9 (-0.2 + 0.2)	$4.6 \pm 1.8$
5.04	$11.4 \pm 1.5$	1.00	5.7 (-0.2 + 0.2)	$7.9 \pm 3.0$
5.09	$8.5 \pm 1.1$	0.94	5.8 (-0.2 + 0.2)	$6.5 \pm 2.4$
5.17	$10.2 \pm 1.3$	0.95	5.6 (-0.2 + 0.2)	$8.7 \pm 3.2$
5.23	$9.1 \pm 1.2$	0.98	5.7 (-0.2 + 0.2)	$8.6 \pm 3.2$
5.27	$9.0 \pm 1.1$	0.90	5.6 (-0.2 + 0.2)	$9.1 \pm 3.3$
5.31	$6.7 \pm 0.9$	0.88	5.7 (-0.2 + 0.2)	$7.3 \pm 2.7$
5.34	$6.8 \pm 0.9$	0.95	5.7 (-0.2 + 0.2)	$7.8 \pm 2.9$
5.39	$15.6 \pm 1.9$	0.91	5.3 (-0.2 + 0.2)	$19 \pm 7$
5.45	$9.0 \pm 1.1$	0.78	5.5 (-0.2 + 0.2)	$12 \pm 5$
5.50	$11.5 \pm 1.4$	0.81	5.4 (-0.2 + 0.2)	$17 \pm 7$
5.56	$17.8 \pm 2.1$	0.80	5.1 (-0.2 + 0.2)	$30 \pm 12$
5.61	$4.2 \pm 0.5$	0.77	5.7 (-0.2 + 0.2)	$7.9 \pm 3.3$
5.65	$8.4 \pm 1.0$	0.71	5.4 (-0.2 + 0.2)	$17 \pm 7$
5.70	$9.5 \pm 1.1$	0.73	5.3 (-0.3 + 0.2)	$21 \pm 9$
5.75	$8.0 \pm 1.0$	0.65	5.3 (-0.3 + 0.2)	$20 \pm 9$
5.79	$6.7 \pm 0.8$	0.74	5.3 (-0.3 + 0.2)	$18 \pm 9$
5.83	$4.4 \pm 0.5$	0.65	5.5 (-0.3 + 0.2)	$13 \pm 7$
5.89	$9.8 \pm 1.2$	0.56	5.1 (-0.3 + 0.3)	$34 \pm 18$
5.96	$5.8 \pm 0.7$	0.51	5.2 (-0.3 + 0.3)	$24 \pm 14$
6.06	$10.5 \pm 1.3$	0.47	4.8 (-0.4 + 0.3)	$62 \pm 38$
6.14	$2.9 \pm 0.3$	0.56	5.2 (-0.5 + 0.3)	$23 \pm 15$
6.19	$4.0 \pm 0.5$	0.49	5.0 (-0.6 + 0.4)	$39 \pm 29$
6.24	$2.2 \pm 0.3$	0.52	5.1 (-0.6 + 0.4)	$28 \pm 22$
6.29	$3.8 \pm 0.5$	0.36	4.8 (-0.8 + 0.4)	$63 \pm 53$
6.38	$3.6 \pm 0.4$	0.35	4.5 (-1.4 + 0.6)	$114 \pm 109$
6.48	$2.1 \pm 0.3$	0.43	4.3 (-3.0 + 0.8)	$195 \pm 195$

paper [16], together with analyses of other high resolution data we have obtained in the decay of the  $T_z = 1/2$  nuclei [17–19]  $^{65}\text{Ge}$ ,  $^{69}\text{Se}$  and  $^{77}\text{Sr}$ .

## 4 Concluding remarks

Compared to previous studies, this work gives new insight into the decay scheme of  $^{73}\text{Kr}$ . Fifteen new gamma emitting states are reported up to an excitation energy of 3469 keV, enriching considerably the level scheme above

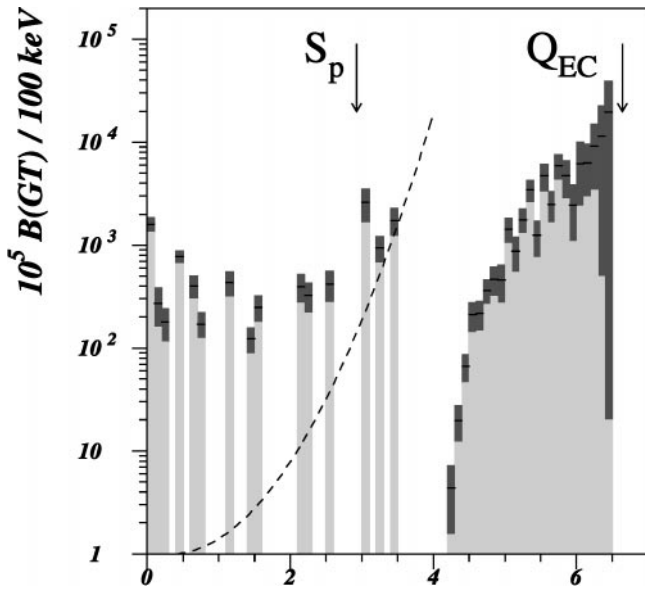


**Fig. 7.** Experimental B(GT) strength distribution for the  $\beta^+$ -EC decay of  $^{73}\text{Kr}$ , binned in 100 keV steps as a function of excitation energy in  $^{73}\text{Br}$ . The dotted line gives an estimate of the lowest B(GT) value accessible to our  $\gamma$  detection. The curve is established from the fluctuation of the registered  $\gamma$  spectra, considering a single  $\gamma$  transition to the lowest possible level and an estimate of the level density [19]. Above 3.5 MeV, no resolved  $\gamma$  lines can be observed and the  $\gamma$  sensitivity vanishes

400 keV of excitation energy. Our measurements confirm the singularly high delayed proton branching of  $^{73}\text{Kr}$  as compared to the other  $T_z=1/2$  precursors in this mass region. In the bell shaped distribution of the delayed particle energy spectrum, several unreported resonance like structures show up.

A spin and parity  $3/2^-$  is assigned to the  $^{73}\text{Kr}$  ground state from our measurements on the basis of the allowed character of the ground state transition, together with the observed allowed decay to the  $5/2^+$  levels located at 286 keV in  $^{73}\text{Br}$ .

From this work, information on Gamow-Teller strength could be obtained up to 97% of the  $Q_{EC}$  energy window. The measured B(GT) distribution is shown in Fig. 7. The gap located in between 3.5 and 4.3 MeV results from a drop of the  $\gamma$  detection efficiency, from spreading of the gamma strength with increasing excitation energy, and from a hindrance of low energy proton emission due to the Coulomb barrier. The limitation introduced by our  $\gamma$  sensitivity indicated by the dotted line (see caption). Above the gap, delayed proton emission allows one to observe beta branches down to an intensity of about  $10^{-6}$  and it can be seen from the histogram that branches of intensity of the order of  $10^{-5}$  contribute significantly to the Gamow-Teller strength at high excitation energy.

According to recent theoretical developments [20–22] total Gamow-Teller strength and its distribution are expected to depend significantly on the shape of the parent nucleus. Such calculations are not yet available for  $^{73}\text{Kr}$ , but it is worth pointing out that two conflicting deformation predictions result from the recent mass estimates of P. Möller et al. [23] ( $\beta_2 = 0.38$ ) and of Y. Aboussir [24] ( $\beta_2 = -0.31$ ). On the experimental side the large  $P_p$  value found in the  $^{73}\text{Kr}$  decay implies an enhancement of the Gamow-Teller strength to the upper part of the  $Q_{EC}$  window by about a factor of 10 in comparison to GT strengths observed in other  $T_z = 1/2$  precursors. This observed feature underlines the need to extend Hartree-Fock Tamm-Dancoff calculations to odd nuclei and specifically to the  $T_z = 1/2$  precursors. Complementary measurements with a total absorption gamma-ray spectrometer would also be highly desirable.

The authors would like to thank Dr. G. Marguier for computing the conversion coefficients.

## References

1. J. Heese, et al. Phys. Rev. **C36**, (1987) 2409
2. J. Heese, et al. Phys. Rev. **C41**, (1990) 1553
3. A.G. Griffiths, et al. Hyperfine Interaction **43**, (1988) 481
4. C. Davids and D.R. Goosman, Phys. Rev. **8**, (1973) 1029
5. E. Roeckl, et al. Z. Physik **266**, (1974) 65
6. P. Asboe-Hansen, et al. Nucl. Phys. **A361**, (1981) 23
7. J.C. Hardy, et al. Nucl. Phys. **A371**, (1981) 349
8. J.B. Mitchell, S. Agami and J.A. Davies, *Radiation Effects*, Vol. 28, (1976) 133
9. Nuclear Data Sheets, Vol.69, n°4 (1993)
10. F. Rösel, et al. Nucl. Data Tables **21**, (1978) 91
11. G. Audi and A.H. Wapstra, Nucl. Phys. **A565**, (1993) 1
12. S. Raman and N.B. Gove, Phys. Rev. **C7**, (1973) 1995
13. M. Satteson, et al. J. Phys. G **16**, (1990) L27
14. D.M. Moltz, et al. Nucl. Phys. **A562**, (1993) 111
15. M. Girod, J.P. Delaroche and D. Gogny, *Nuclear Structure in the nineties*, April 1990, Oak Ridge
16. J. Giovinazzo, Ph. Dessagne, Ch. Miehé (to be published)
17. Ph. Dessagne, et al. Phys. Rev. **C37**, (1988) 2687
18. Ph. Dessagne, Ph.D. Thesis, University Louis Pasteur of Strasbourg, France 1987
19. J. Giovinazzo, Ph.D. Thesis, University Louis Pasteur of Strasbourg, France 1997
20. I. Hamamoto and X.Z. Zhang, Z. Phys. **A353**, (1995) 145
21. F. Frisk et al., Phys. Rev. **C52**, vol5, (1995) 2468
22. P. Sarriguren et al., Nucl. Phys. **A635**, (1998) 55
23. P. Möller, J.R. Nix, W.D. Myers, W.J. Swiatecki, Nucl. Data Tables **59**, (1995) 185
24. Y. Aboussir, Atomic Data and Nuclear Data Tables **61**, (1995) 127